

# Alpha–Beta Transition in Poly(butylene terephthalate) As Revealed by Small-Angle X-ray Scattering

Anton A. Apostolov,<sup>\*,†,‡</sup> Stoyko Fakirov,<sup>†</sup> Manfred Stamm,<sup>‡</sup> Rahul D. Patil,<sup>§,#</sup> and James E. Mark<sup>§</sup>

Laboratory on Structure and Properties of Polymers, Department of Chemistry, Sofia University, 1 J. Bourchier Blvd., 1126 Sofia, Bulgaria; Institut für Polymerforschung Dresden e. V., Hohe Strasse 6, 01069 Dresden, Germany; Department of Chemistry and the Polymer Research Center, University of Cincinnati, Cincinnati, Ohio 45221-0172; and Max-Planck-Institut für Polymerforschung, Postfach 3148, 55021 Mainz, Germany

Received February 24, 2000; Revised Manuscript Received June 13, 2000

**ABSTRACT:** The stretching-induced alpha–beta polymorphic transition in the crystalline regions of poly(butylene terephthalate) (PBT) is studied by small-angle X-ray scattering (SAXS), instead of by the wide-angle X-ray scattering (WAXS) usually used for this purpose. An expression for the increase of the long spacing upon the transition is derived from a simple model of oriented PBT as a set of microfibrils, each consisting of alternating crystalline and amorphous regions. This increase is calculated on the basis of the *c* unit cell parameter of both alpha and beta phases and the degree of crystallinity as obtained from differential scanning calorimetry. There is a fairly good agreement between this value and the experimentally measured one. The affine deformation model holds for both the alpha and beta phases in the whole interval of the strain, from zero up to the strain at break. Without external stress the microfibrils are in the fully relaxed state, as concluded from the values of the corresponding long spacing (from SAXS) comprising exclusively the alpha modification (from WAXS). Both the polymorphic transition and the change in the long spacing with strain are completely reversible in the deformation range investigated.

## Introduction

It is well-known that crystalline poly(butylene terephthalate) (PBT) in the relaxed state exists in the so-called alpha form, whereas the alternative beta form is observed only when the sample is held under strain.<sup>1–11</sup> These two forms are characterized by different parameters of the unit cell. The molecular chain in the alpha form is not fully extended, and the glycol residues are in the gauche–trans–gauche conformation, whereas in the beta form it is fully extended with the glycol residues in the trans–trans–trans conformation. These differences in conformation primarily affect the unit cell parameter *c*, which changes abruptly from 11.65 to 12.90 Å in going from the alpha to the beta form.<sup>11</sup> This parameter is the most sensitive to the transition and hence is often used to detect the transition. The planes (–104) and (–106) are almost perpendicular to the *c*-axis, and thus the corresponding changes in the *d*-spacings in the course of the external deformation can be used to identify the alpha–beta transition. More specifically, several authors<sup>1,3,10,12</sup> use the stress- or strain-induced shift of the (–104) WAXS reflection from 31.2° to 28.3° in  $2\theta$  (for Cu K $\alpha$  radiation) brought about by the transition. Changes in the infrared spectra in the transition region were also considered,<sup>9</sup> and Ward and Hall<sup>13</sup> used Raman spectroscopy for the same purpose. Some more unusual methods such as differential scanning calorimetry (DSC) under tension<sup>6</sup> or changes in the microhardness under strain<sup>14</sup> were also

used for following the transition. Since the alpha form exists below a certain strain and the beta form only above it, the transition is fully reversible.

In a thorough study of this polymorphic transition in PBT, Tashiro et al.<sup>6</sup> used small-angle X-ray scattering (SAXS) measurements, DSC measurements under tension, quantitative analysis of infrared spectra, and evaluations of crystallite sizes in (–104) direction by WAXS. They followed the changes in the long spacing as dependent on both the strain and the stress and found an S-shaped dependence in the latter case, which allows precise determination of the transition region. They also found that the long spacing increased approximately in proportion to the strain, in the absence of a kink.<sup>6</sup> For this reason precise determination of the transition region (as expressed as percent strain) is not possible. Also, Tashiro et al.<sup>6</sup> did not state if the long spacing had been calculated on the basis of the maximum position or the center of gravity position. This is an important point, since much higher precision may be reached in the latter case.

This earlier work encouraged the present investigation, the aim of which was to develop a method for detecting and following the alpha–beta transition in PBT by the strain dependence of the long spacing as revealed by SAXS.

## Experimental Part

**Samples.** The samples of PBT (melt index = 50) were obtained from the Aldrich Chemical Co. Bristles having approximate diameters of 1 mm were obtained using a modular flow index apparatus (MFI-6542, Donau Electronics, Switzerland). The melt was kept in the barrel for ca. 10 min and subsequently extruded through the nozzle (1 mm diameter) into ice-cold water by applying a constant force of 220 N to the plunger. The bristles were drawn through neck formation  $3.3\times$  at room temperature by means of a Zwick mechanical

<sup>†</sup> Sofia University.

<sup>‡</sup> Institut für Polymerforschung Dresden e. V.

<sup>§</sup> University of Cincinnati.

<sup>‡</sup> Max-Planck-Institut für Polymerforschung.

<sup>#</sup> Present address: Department of Materials Science and Engineering, Pennsylvania State University, University Park, PA 16802.

\* To whom all correspondence should be addressed.

testing machine and were then annealed at constant length for 6 h at 180 °C under vacuum. This was done to obtain higher crystallinity and thus to improve the quality of the X-ray data, obtained as described below.

**X-ray Measurements.** The SAXS measurements were performed with pinhole collimation on an 18 kW rotating-anode generator using Cu K $\alpha$  radiation. An area gas detector with 512  $\times$  512 pixels and 0.117 mm spatial resolution in each direction was used, and the sample-to-detector distance was set to 119 cm. The acquisition time was 1 h. Each measurement under stress was immediately followed by another in the absence of stress (in the relaxed state), before applying the additional stress required for a larger deformation. The deformation or strain was defined by  $\epsilon = (l - l_0)/l_0$ , where  $l_0$  was the initial length between two marks on the bristle and  $l$  was the length between the same marks at deformation  $\epsilon$ . Both the deformation under stress and the residual deformation (in the absence of stress) were read. 2D patterns were obtained and processed by means of *General Area Detector Diffraction Software* from Siemens. The data were corrected for background scattering, detector efficiency, and counting time. No correction for the change of the sample diameter with the deformation was made since it affects to a first approximation only the intensity but not the location of the peak. Meridional cuts were taken through the 2D patterns and Lorentz corrected by multiplying the intensity  $I(s)$  by  $s^2$ , where  $s = 2 \sin \theta/\lambda$  is the wave vector. The meridional cuts of the 2D patterns consist of two symmetrical maxima above and below the beam stopper. To obtain higher precision in determination of the long spacing, the center of gravity of the  $I(s)s^2$  vs  $s$  curve was used for both maxima, and the average value was taken. The long spacing for a single maximum was calculated as the reciprocal value of the  $s$ -coordinate of the first moment of the intensity distribution:

$$L = \sum I(s)s^2 / \sum I(s)s^3 \quad (1)$$

where the summation was taken in the vicinity of the maximum in order to avoid the tails which were, at least in some cases, relatively high.

The WAXS measurements were performed on a standard Siemens D500 diffractometer with Cu K $\alpha$  radiation and Ni-beta filter in transmission mode. Since the goal was only to compare the full width at half-height (fwhh) of certain maxima of the initial sample and the sample after break, no correction for the instrumental enlargement of the maxima was made.

**DSC Measurements.** These measurements were conducted in a Mettler DSC-30 calorimeter using a heating rate of 10 °C/min in the temperature range -40 to 250 °C under an argon atmosphere. The glass transition and the melting temperatures were evaluated from the built-in software package. The degree of crystallinity  $w_c$  was calculated from the commonly used ratio of the measured  $\Delta H$  to the ideal heat of fusion  $\Delta H_0 = 96.4$  kJ/kg;<sup>15</sup>  $w_c = \Delta H/\Delta H_0$ .

## Results and Discussion

The dependence of the long spacing  $L$  on deformation is shown in Figure 1, for both the total deformation ( $\epsilon$ , empty circles) and the residual deformation ( $\epsilon_r$ , filled circles). The long spacing measured under stress  $L$  (empty circles) increases from 100 to 109 Å with total relative deformation  $\epsilon$  going from 0 to 9%. An important point here is that further increase in  $\epsilon$  results in a kinkwise change in  $L$ ; thereafter,  $L$  increases linearly again with  $\epsilon$  up to 120 Å, with the fiber rupture for  $\epsilon > 16\%$ .

The values of  $L$  in the relaxed state (filled circles) are all approximately equal to the initial value of  $L_0$  of 100 Å. The highest residual deformation obtained is 3.8% after a total deformation of 16%. The two continuous lines in Figure 1 are drawn according to least-squares method (LSM) through points 0–2 and 3–6. The dashed

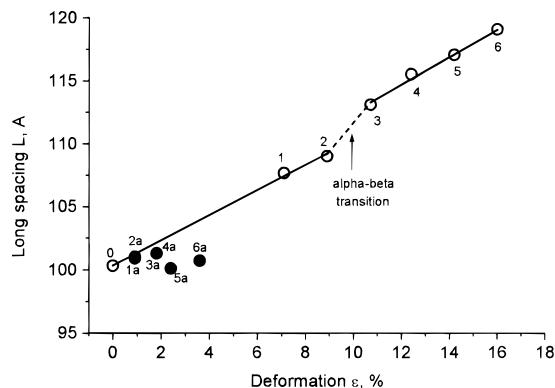


**Figure 1.** Dependence of the long spacing  $L$  on the deformation  $\epsilon$ . The filled circles represent the long spacing in the absence of stress and are taken after the measurements under the respective strain.

line in the deformation range 9–11% reflects the alpha-beta transition. Since there is a distribution of stress across the cross section of the bristle, not all microfibrils undergo the transition simultaneously, and for this reason, the observed transition is not abrupt.

For the case of affine deformation the relative change of the long spacing is proportional to the external deformation  $\epsilon$ , i.e.,

$$(L - L_0)/L_0 = (l - l_0)/l_0 = \epsilon/100, \quad [\epsilon] = \% \quad (2)$$

Hence, the long spacing increases linearly with  $\epsilon$ :

$$L = L_0 + k\epsilon \quad (3)$$

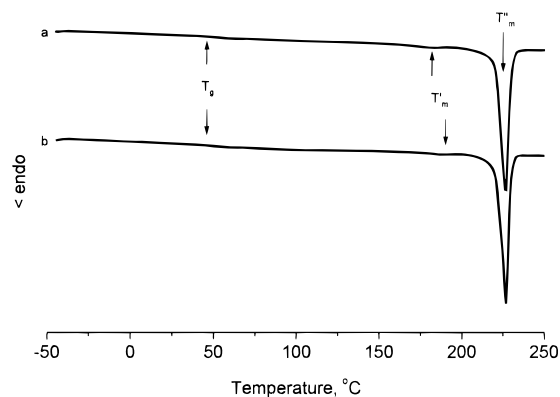
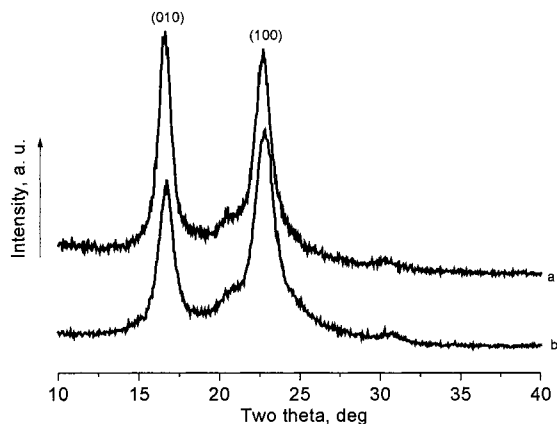
where  $L_0$  is the intercept and  $k = L_0/100$  is the slope. This suggested an LSM fitting through points 0–2 but this time under the constraints of eq 3 (a certain intercept and slope equal to the intercept/100). Table 1 presents the results of this fitting, reflecting the affine deformation model, as well as the results from a simple LSM fit (i.e., without any constraints). For both fits the results coincide within experimental error. This indicates that the PBT sample under investigation (comprising exclusively of the alpha phase in the crystalline regions) elongates affinely for deformations from zero up to the transition region.

To check whether the same sample also deformed affinely after the polymorphic transition, i.e., when the crystallites comprise the beta phase, points 3–6 in Figure 1 were considered. Point 3 was taken as a basis to monitor the deformation of the beta phase. A fit through points 3–6 according to LSM, both without any constraints and with the constraints of eq 3 was performed. The results of these two fits are also given in Table 1. For both fits the results coincide within experimental error. It follows that the sample comprising exclusively of the beta phase in the crystalline regions elongates affinely as well. Notice that in this case the intercept  $L_0$  differs from the basic value of  $L = 113.2$  Å for zero deformation of the beta phase (or total deformation of 10.7%, Figure 1).

Figure 2 shows the thermograms a and b of the initial sample and of the sample after its rupture at deformation higher than 16%, respectively. Since after the rupture the microfibrils relax, the measurements in both cases (curves a and b) were carried out with samples in the relaxed state, when the crystalline PBT is in the alpha modification (as will be shown below).

**Table 1. Intercept  $L_0$ , Slope  $k$ , and Correlation Coefficient  $R$  for the Elongation of Fibers Containing Alpha and Beta Forms of Crystalline PBT**

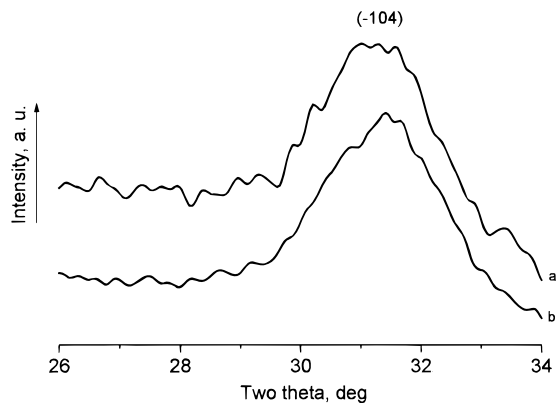
parameter	alpha form			beta form		
	$L_0/\text{\AA}$	$k/\text{\AA \%}^{-1}$	$R$	$L_0/\text{\AA}$	$k/\text{\AA \%}^{-1}$	$R$
from linear regression	$100.3 \pm 0.3$	$0.99 \pm 0.04$	0.999	$101.6 \pm 1.1$	$1.09 \pm 0.07$	0.996
from affine deformation	$100.3 \pm 0.13$	1.00 (fixed)	0.999	$102.8 \pm 0.2$	1.00 (fixed)	0.996

**Figure 2.** Thermograms of the initial oriented PBT sample (a) and the broken sample after its rupture at a deformation larger than 16% (b).**Figure 3.** Equatorial diffractograms of the initial oriented sample (a) and the broken sample after its rupture at a deformation larger than 16% (b).

One purpose of Figure 2 is to permit comparisons of curves a and b to see whether any changes, detectable with DSC, occur in the sample after the alpha–beta–alpha transition. The corresponding degrees of crystallinity by weight are for the initial sample (curve a)  $w_c = 0.67$  and for the sample after the rupture (curve b)  $w_c = 0.64$ . The results indicate that DSC cannot detect structural changes taking place in a sample during the alpha–beta transition followed by additional stretching, rupture, and subsequent relaxation of the stress (upon which the alpha modification reappears). In addition, as seen from the same figure, the glass transition temperatures are the same for the two samples.

The equatorial diffractograms a and b of the initial sample and of the sample after its rupture at deformation higher than 16%, respectively, are shown in Figure 3. The only difference between the two curves is the reflections in curve b being larger than those in curve a. This may be attributed to increased imperfections of the crystallites in the ruptured sample.

The corresponding meridional diffractograms a and b are shown in Figure 4. Again, as in Figure 3, the reflections in curve b are broader than in curve a, which

**Figure 4.** Meridional reflex (–104) of the initial oriented (a) and the broken sample after its rupture at deformation larger than 16% (b).

can be attributed to the same imperfections. Generally, some residual stress after rupture could be expected and subsequently part of the crystallites would possibly have been in beta modification. This was not the case here, however, since for both samples the angular position of the (–104) reflex is  $31.2^\circ 2\theta$  (Figure 4), which means that the crystallites are in the alpha modification.

From all of these data, the following model for the structural changes which take place upon deformation of the bristle may be suggested. The deformation region can be divided into three intervals, each involving a different mechanism. In the first deformation interval, in the initial state ( $\epsilon = 0$ ), the crystalline PBT is in alpha modification. With increase in strain (Figure 1), the tie molecules occupying amorphous regions stretch, and under a specific strain (8.9% in our case), most of them reach full length. It is noteworthy that in this deformation interval ( $\epsilon = 0$ –8.9%) the stress applied is experienced only by the chain segments in the amorphous regions; i.e., the crystallites remain unaffected. The bristle deforms affinely (see Figure 1 and Table 1).

In the second deformation interval ( $\epsilon = 8.9$ –10.7%), conformational changes take place mostly in the crystallites, and the alpha–beta transition occurs in the crystalline regions. Stepwise increase of the long spacing from 108 to 112 Å (dashed line in Figure 1) can be seen as a result of this polymorphic transition. At the following, higher deformation the transition is practically completed. This follows from previous investigations,<sup>1,4,7,14</sup> performed by WAXS or microhardness measurements.<sup>14</sup> In Jakeways et al.'s investigations<sup>1,4</sup> the transition starts at 4 and is completed at 10–13% strain. According to Yokouchi et al.,<sup>7</sup> both modifications coexist at 12% strain whereas only beta modification remains for higher strains. Our investigations show that the transition takes place in the strain interval between 5.3 and 12.9%.<sup>14</sup> Unfortunately, the step in the strain value used in the previous study<sup>14</sup> is too large to allow more precise determination of the transition conditions. More specifically, the polymorphic transition takes place in a relatively large deformation interval due to both distribution of the stress and some peculiarities of the



**Table 2. Full Width at Half-Height (fwhh) of Some Reflections of the Alpha Form of PBT before and after the Rupture of the Fiber**

sample	initial oriented sample			oriented sample after rupture		
reflex	(010)	(100)	(-104)	(010)	(100)	(-104)
fwhh, rad	0.0166	0.0226	0.0431	0.0183	0.0252	0.0494

method used for its identification. From all these considerations it follows that in point 3 (Figure 1) the transition is almost entirely completed; the crystallites are in the beta form, and the tie molecules are fully stretched. This second deformation interval is characterized with an abrupt, kinkwise increase of the long spacing, according to a different mechanism relative to that in the first interval.

In the third deformation interval, again an affine increase of the long spacing can be seen. As already stated, a substantial part of the tie molecules are stretched, and further increase of the deformation leads to a stress in the crystallites and subsequent pull-out of some of these molecules. This is in agreement with the observed increase in the degree of imperfection of the crystallites, as can be concluded from the enlargement of the lines (010), (100) (Figure 3), and (-104), (Figure 4, compare curves a and b; see also Table 2). The pulling out takes place simultaneously with the stretching of a part of the tie molecules, which have not yet reached full length. It is worth noticing that this effect hardly affects the DSC degree of crystallinity (Figure 2). It seems that only some chains can be pulled out from the crystallites, and when they are also stretched, rupture of the entire bristle occurs (Figure 1, to the right, from point 6). Such pulling out of molecules from the PBT crystallites has already been shown to occur upon deformation for poly(ether ester)s based on PBT as hard segments and poly(ethylene oxide) as soft segments.<sup>16</sup>

The results for the residual deformation at least partially support this model. For total deformations up to 8.9% (point 2, Figure 1) the value of the residual long spacing is close to the initial value (points 1a and 2a), and this is because the deformation in this range is due exclusively to the stretching of chains in the amorphous regions. Since the stretching is reversible, the change of the long spacing is reversible, too. The long spacing in the relaxed state after the polymorphic transitions is also equal to the initial value (point 3a, Figure 1) since the polymorphic alpha-beta transition is reversible. Points 4a-6a, though, should lie higher, since in this region irreversible pulling out of chains with the progress of deformation occurs, and the long spacing also increases partially irreversibly.

Let us imagine the long spacing for the alpha modification  $L^\alpha$  as a sum of the average thickness of the crystallites  $l_c^\alpha$  and the average size of the amorphous regions  $l_a^\alpha$ . By analogy,  $L^\beta = l_c^\beta + l_a^\beta$ . Since the polymorphic transition concerns only the crystalline regions, in the transition interval the size of the amorphous region remains constant, i.e.,  $l_a^\alpha = l_a^\beta$ . Each crystalline region comprises several crystallites all oriented with the  $c$ -axis parallel to the fiber axis; hence

$$l_c^\beta/l_c^\alpha = c^\alpha/c^\beta \quad (4)$$

where  $c^\alpha$  and  $c^\beta$  are the respective unit cell parameters. On the other hand, on the assumption that all polymeric material is situated in microfibrils, representing alternating crystalline and amorphous regions,  $l_c^\alpha$  is con-

nected with  $L^\alpha$  through the linear degree of crystallinity by volume  $v_c$ :

$$l_c^\alpha = v_c L^\alpha \quad (5)$$

By combining all the above equations, it follows that

$$L^\beta = L^\alpha \{ v_c [(c^\beta/c^\alpha) - 1] + 1 \} \quad (6)$$

The crystallinity by volume  $v_c$  is related to the crystallinity by weight  $w_c$  as<sup>17</sup>

$$v_c = \rho w_c / \rho_c \quad (7)$$

where  $\rho$  is the mean density. In the present case it can be calculated from

$$w_c = \rho_c (\rho - \rho_a) / \rho (\rho_c - \rho_a) \quad (8)$$

Desborough and Hall<sup>11</sup> summarized the results of several authors on the unit cell parameters of the alpha and beta forms of PBT and suggested  $c_\alpha = 11.65$  and  $c_\beta = 12.90$  Å as the best available values. Using these values and  $w_c = 0.67$ , on the basis of eq 6 an increase of 6.9% in the long spacing can be expected as a result of the alpha-beta transition. The experimentally observed increase is only 3.7% (calculated from point 2 to point 3, Figure 1). One possible explanation for this discrepancy is that the stress distribution (i.e., unequal stresses in the microfibrils at the same time) leads to a deformation interval for the transition that is even larger than observed. Consequently, the change in the long spacing will be larger and closer to the value 6.9% calculated on the basis of eq 6. The presence of a part of the amorphous material in the interfibrillar space will also complicate the matter since the linear degree of crystallinity (used in eq 6) will differ from the bulk crystallinity (calculated from DSC).

## Conclusions

SAXS was successfully used to detect the polymorphic alpha-beta transition in PBT under the strain. It was found that the deformation of both the alpha and beta phases follows the affine deformation model but involves different molecular mechanisms. The affine deformation in the alpha phase is due to the stretching of the tie molecules upon deformation. The affine deformation in the beta phase is believed to be due to the pulling out of macromolecules from the beta form crystallites, as well as to additional stretching of tie molecules. The microfibrils were found to fully relax after removal of the stress. Further, the changes in long spacing in these two cases are completely reversible since the conformational changes in the amorphous region are reversible. The stepwise change in the long spacing during the polymorphic transition in a relatively narrow deformation interval is also reversible, due to the reversibility of this transition. Finally, a new method of calculating the kinkwise increase of the long spacing in the polymorphic transition region was proposed.

**Acknowledgment.** The partial support of BMBF, Germany, Project BUL-035-97, and a NATO collaborative grant is highly appreciated. A.A.A. expresses his gratitude for the hospitality of Max-Planck-Institut für Polymerforschung, Mainz, Germany, where some of the experiments were carried out.

## References and Notes

- (1) Jakeways, R.; Smith, T.; Ward, I. M.; Wilding, M. A. *J. Polym. Sci., Polym. Lett. Ed.* **1976**, *14*, 41–46.
- (2) Mencik, Z. *J. Polym. Sci., Polym. Phys. Ed.* **1975**, *13*, 2173–2181.
- (3) Brereton, M. G.; Davis, G. R.; Jakeways, R.; Smith, T.; Ward, I. M. *Polymer* **1977**, *19*, 17–26.
- (4) Jakeways, R.; Ward, I. M.; Wilding, M. A.; Hall, I. H.; Desborough, I. J.; Pass, M. G. *J. Polym. Sci., Polym. Phys. Ed.* **1975**, *13*, 799–813.
- (5) Hall, I. H.; Pass, M. G. *Polymer* **1975**, *17*, 807–816.
- (6) Tashiro, K.; Nakai, Y.; Kobayashi, M.; Tadokoro, H. *Macromolecules* **1980**, *13*, 137–145.
- (7) Yokouchi, M.; Sakakibara, Y.; Chatani, Y.; Tadokoro, H.; Tanaka, T.; Yoda, K. *Makromolecules* **1976**, *9*, 266–273.
- (8) Roebuck, J.; Jakeways, R.; Ward, I. M. *Polymer* **1992**, *33*, 227–232.
- (9) Tashiro, K.; Hiramatsu, M.; Ii, T.; Kobayashi, M.; Tadokoro, H. *Sen-I Gakkashi* **1986**, *42*, 597–605.
- (10) Tashiro, K.; Hiramatsu, M.; Ii, T.; Kobayashi, M.; Tadokoro, H. *Sen-I Gakkashi* **1986**, *42*, 659–664.
- (11) Desborough, I. J.; Hall, I. H. *Polymer* **1977**, *18*, 825–830.
- (12) Nakamae, K.; Kameyama, M.; Yoshikawa, M.; Matsumoto, T. *J. Polym. Sci., Polym. Phys. Ed.* **1982**, *20*, 319–326.
- (13) Ward, I. M.; Hall, I. H. *Polymer* **1977**, *18*, 327–337.
- (14) Fakirov, S.; Boneva, D.; Balta Calleja, F. J.; Crumova, M.; Apostolov, A. A. *J. Mater. Sci. Lett.* **1998**, *17*, 453–457.
- (15) *Polymer Data Handbook*; Mark, J. E., Ed.; Oxford University Press: New York, 1999; p 350.
- (16) Fakirov, S.; Fakirov, C.; Fischer, E. W.; Stamm, M. *Polymer* **1991**, *32*, 1173–1180.
- (17) Vonk, C. G. Experimental Practice. In *Small Angle X-ray Scattering*; Glatter, O., Kratky, O., Eds.; Academic Press: London, 1982; p 454.

MA000338D